A Combined Experimental and Theoretical Evaluation of the Structure of Hydrated Microporous Aluminophosphate $AlPO_4$-18

G. Poulet,[†,‡] A. Tuel,[‡] and P. Sautet*[,†]

Laboratoire de Chimie, UMR 5182 CNRS, Ecole Normale Supérieure de Lyon, 46 allée d'Italie, 69364 Lyon Cedex 07, France, and Institut de Recherches sur la Catalyse, UPR 5401 CNRS, 2 avenue Albert Einstein 69626 Villeurbanne Cedex, France

Received: February 7, 2005; In Final Form: June 20, 2005

Water adsorption in the microporous aluminophosphate $AlPO_4$-18 is studied by a combination of solid-state NMR, X-ray diffraction, and density functional theory calculations. The change of the framework structure upon hydration is moderate, and NMR gives local information on the environment of Al and P atoms. The structural distribution of water molecules in the channels has been explored by a combination of first-principle molecular dynamics simulations and of static geometry optimizations. Two starting points have been considered for the calculations. If the structure of the dehydrated aluminophosphate is used, the simulation result is not satisfactory with an incomplete hydration and no agreement with NMR results. Starting from a partial refinement of the aluminophosphate framework for the hydrated system, a structure with six tetrahedral and six octahedral Al atoms in the unit cell is obtained, involving twelve water molecules coordinated to Al atoms and twelve others in the channels, and in good agreement with experimental data.

Introduction

Since their discovery in 1982 by Flanigen and co-workers,[1,2] crystalline microporous aluminophosphates ($AlPO_4$-*n*) have received considerable attention due to their properties similar to those of zeolites. Their structure consists of corner-sharing AlO_4 and PO_4 tetrahedra, forming pores and cavities of molecular dimension, and making them particularly attractive in adsorption and molecular sieving. Moreover, substituted networks (MeAPO, SAPO, and MeAPSO) are potentially interesting as heterogeneous catalysts for acidic or oxidation reactions.[3−5]

Many structures with different pore sizes and architectures can be obtained by changing the nature of the reagents or the experimental conditions such as the gel composition, the crystallization temperature, or the crystallization time.[6,7]

The channels of as-made aluminophosphates are generally filled with organic molecules occluded during crystallization. In most cases, the molecules can be removed by calcination in air at high temperature. When the calcined compound is contacted with air at room temperature, water molecules penetrate the channels and can modify the coordination of framework aluminum species. First observed on $AlPO_4$-5, $AlPO_4$-11, $AlPO_4$-17, and $AlPO_4$-31, this change in coordination is often accompanied by a reversible structure deformation.[8] ^{27}Al solid-state NMR is a particularly efficient tool to study these modifications, the chemical shift of aluminum atoms being very sensitive to their coordination.[9] Interactions between water molecules and framework atoms have been studied by this technique in $AlPO_4$-5,[10,11] $AlPO_4$-11,[12] $SAPO_4$-34,[13] and VPI-5.[14−17] NMR can be combined with other experimental techniques such as X-ray diffraction,[18−25] infrared spectroscopy (IR),[26,27] neutron diffraction,[28] or diffuse reflectance spectroscopy[29] to better define the topology of the hydrated materials.

However, an experimental approach is often not sufficient to describe precisely the hydrated structure of the aluminophosphate, in particular the position of hydrogen atoms. We have recently reported that a theoretical approach based on first principles calculations could bring additional information on the position and the dynamics of water molecules in the channels of hydrated $AlPO_4$-34.[30]

$AlPO_4$-18 (**AEI** framework topology) and the corresponding substituted materials (SAPO-18 and MeAPO-18, Me = Mg, Zn, Co) have been used as molecular sieves and as catalysts in the methanol-to-olefin conversion.[31−33] The structure of the calcined never-rehydrated aluminophosphate has been solved from the refinement of synchrotron powder diffraction data.[34] The pattern was indexed in the monoclinic space group *C*2/*c* with $a = 13.711$, $b = 12.731$, $c = 18.570$ Å, and $\beta = 90.01°$. The framework topology of $AlPO_4$-18 is shown in Figure 1.

The framework consists of layers of double 6-ring (D6R) units, which are the same as those in the $AlPO_4$-34 (**CHA** framework type). These layers are tilted in $AlPO_4$-18 but not in the chabazite structure, leading to a pear-shaped cage with six 8-rings and twelve 4-rings. As for $AlPO_4$-34, the calcined structure is modified upon hydration. The structural changes have been studied not only by X-ray diffraction and solid-state NMR[35] but also by calorimetry and IR.[36,37] Attempts to solve the hydrated structure from X-ray powder diffraction profiles were not successful. Various unit cells have been proposed, but none of them correctly indexes the X-ray pattern.

The aim of the present work is to combine DFT calculations with experimental methods to get insights on the calcined rehydrated form of $AlPO_4$-18.

* To whom correspondence should be addressed. E-mail: Philippe.Sautet@ens-lyon.fr.
† Ecole Normale Supérieure de Lyon.
‡ Institut de Recherches sur la Catalyse.

10.1021/jp050670x CCC: $30.25
Published on Web 11/08/2005

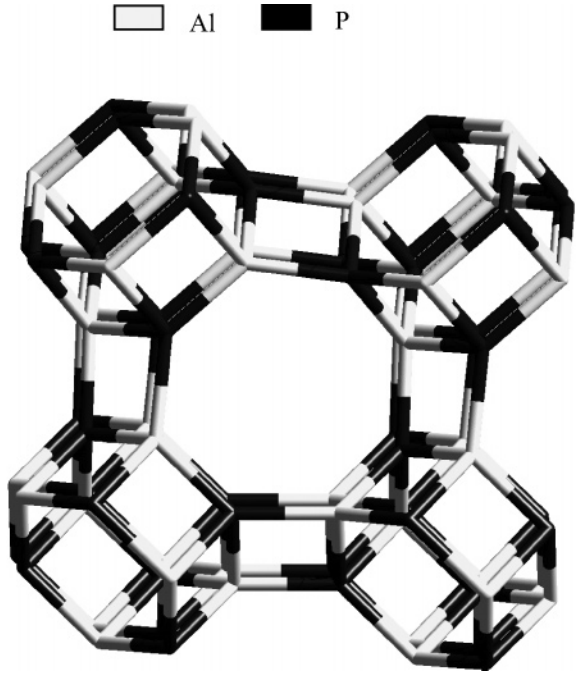

Figure 1. Calcined-never-rehydrated $AlPO_4$-18 (framework oxygen atoms omitted) showing the tridimensional elliptical open eight-member-ring channel.

Methods

1. Computational. The total energy and structure of the calcined rehydrated form of $AlPO_4$-18 were determined using the Vienna ab initio simulation program (VASP).[38−42] This code solves the Kohn−Sham equation of density functional theory for periodic systems, developing the one-electron wave function on a basis set of plane waves. The density functional was parametrized in the local-density approximation (LDA), with the exchange correlation functional proposed by Perdew and Zunger[43] and corrected for nonlocality in the generalized gradient approximation (GGA) using the formulation of Perdew and Wang.[44,45] The electron−core interactions were described with the projector-augmented wave method, which is a frozen core approach using the exact valence instead of pseudowave function in the classical pseudopotential framework.[46,47] An energy cutoff of 500 eV for the plane waves was selected in order to minimize the influence of Pulay stress, arising from basis set incompleteness, for the optimization of the unit cell shape.[48] Tests with a larger number of K points showed that, due to the great size of this unit cell, Γ-point calculations are precise enough to obtain convergence of the structure and energy. The FFT grid has a size of 70 × 70 × 140, and the projection operators for the pseudopotentials are evaluated in real space. A conjugate gradient procedure is used to relax the ions into their optimum structure. The ionic relaxation is terminated with a change in the total free energy smaller than 10^{-4} eV. An important point for our calculation method is that no symmetry conditions were imposed during the relaxation.

This code has been already used on $AlPO_4$-34 (**CHA** topology)[30] and calcined $AlPO_4$-18,[49] with similar computational settings as here. The calculated calcined dehydrated $AlPO_4$-34 and $AlPO_4$-18 were in excellent agreement with the experimental data with an average deviation for the atomic coordinates of 0.03 Å and of 0.3% for the lattice vectors in the case of $AlPO_4$-34. The calculated cell parameters for calcined dehydrated $AlPO_4$-18 are $a = 13.903$ Å, $b = 12.903$ Å, $c = 18.833$ Å, $\alpha = \gamma = 90°$, and $\beta = 89.89°$. The two simulated X-ray powder diffraction patterns of the optimized and experimental structures were perfectly correlated. The only difference between the two patterns was that peaks for the calculated structure were slightly displaced toward low angle values. This was explained by a well-known tendency of DFT-GGA to slightly overestimate atomic distances and cell volume.

Fixed-volume Born Oppenheimer molecular dynamics runs were conducted in simulated canonical ensemble using the algorithm of Nosé.[50,51] A Verlet velocity algorithm[52] was used to integrate Newton's equations of motion with a time step of 0.5 fs. The runs were performed at 300 K for periods ranging from 0.2 to 0.5 ps. A procedure which alternates geometry optimizations and molecular dynamics runs was set up in order to increase the speed of coordination of water molecules on some aluminum atoms and to reach an optimal structure for the hydrated AlPO.

Lazy Pulverix[53] software was used to simulate X-ray powder diffraction patterns of $AlPO_4$-18. The validity of the simulation program was evaluated on the calcined dehydrated $AlPO_4$-34, for which the simulated X-ray powder pattern was compared with the experimental one. Both the position and the intensity of the reflections were strictly the same for the two patterns.

2. Experimental Details. $AlPO_4$-18 was synthesized hydrothermally following a procedure reported by Simmen et al.[34] A gel with the following molar composition $0.33HCl-0.675(TEA)_2O-Al_2O_3-P_2O_5-35H_2O$ was prepared using Pseudoboehmite (CATAPAL B, Vista, 74 wt % Al_2O_3), phosphoric acid (85 wt % in water), tetraethylammonium hydroxide (TEAOH, 25 wt %, Aldrich), hydrochloric acid (37 wt % in water), and water. Crystallization was carried out under static conditions at 150 °C for 7 days in a Teflon-lined stainless steel autoclave. The as-synthesized material was recovered by centrifugation, washed with distilled water, and dried at 100 °C overnight. The organic template occluded within the $AlPO_4$-18 channels was removed by calcination in air. The as-made solid was first heated at 200 °C (heating rate = 1 °C min^{-1}) for 3 h. The temperature was then slowly increased to 500 °C (heating rate = 0.6 °C min^{-1}), and the solid was kept at that temperature for 24 h. The rehydrated $AlPO_4$-18 was obtained by contacting the calcined never-rehydrated solid with ambient moisture for 24 h.

3. Characterization. X-ray Powder Diffraction. Powder X-ray diffraction patterns of the as-synthesized and calcined-rehydrated forms of $AlPO_4$-18 were recorded on a Bruker D5005 diffractometer using the Cu Kα radiation. Data were collected under ambient conditions between 3 and 80° (2θ) with a step size of 0.02° and a counting time of 10 s per step.

Thermogravimetric Analysis (TGA). TGA of the calcined rehydrated material was performed using a Mettler TA3000 system in the temperature range between 20 and 200 °C with a heating rate of 0.2 °C min^{-1}.

Solid-State NMR. All solid-state NMR experiments were performed on a Bruker DSX 400 spectrometer operating at 104.25 and 161.1 MHz for ^{27}Al and ^{31}P nuclei, respectively. Conventional magic-angle spinning (MAS) NMR spectra were recorded using a double-bearing probe head equipped with 4-mm (outside diameter) zirconia rotors. Samples were spun at the magic angle with a spinning speed of 14 kHz. The pulse lengths were 2 μs ($\pi/4$) and 0.7 μs ($\pi/6$), and the recycle delays were 30 and 1 s for ^{31}P and ^{27}Al nuclei, respectively. Two-dimensional 5-quanta (2D-5Q) MAS NMR spectra were collected with a standard 4-mm probe head at a spinning speed of 11 kHz and a RF field of 175 kHz, using a modified RIACT sequence,[54,55] already used for the study of $AlPO_4$-34.[21] ^{27}Al

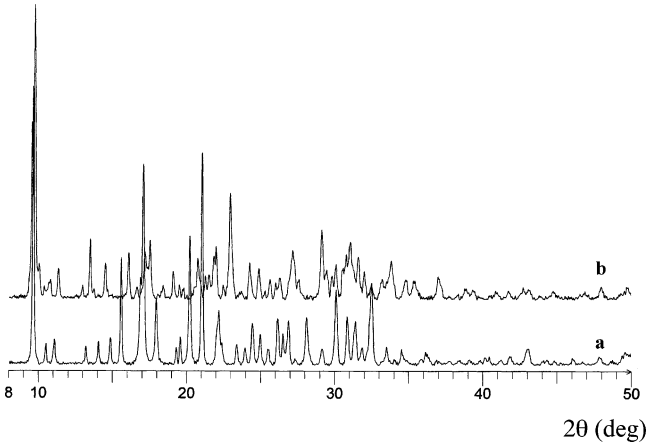

Figure 2. X-ray diffraction powder pattern of $AlPO_4$-18. (a) As-synthesized $AlPO_4$-18. (b) Calcined-rehydrated $AlPO_4$-18.

→ ^{31}P CP/MAS experiments were performed using a three-channel ^{1}H−X−Y probe head (Bruker) and a conventional spin-lock sequence.[56] Encoding the aluminum evolution frequencies in an initial time period after the 90° pulse performed two-dimensional ^{27}Al → ^{31}P CP/MAS correlation experiments. Pure absorption-phase NMR line shapes in both dimensions were obtained by cycling phase of the 90° pulse using the TPPI scheme.[57,58] The Hartmann−Hahn matching condition,[59] modified to take only the central ^{27}Al transition into account, was set up experimentally on the rehydrated $AlPO_4$-18 sample. A more homogeneous transfer was achieved by linear amplitude modulation of the spin-locking field on the aluminum.[60] The contact time was 1.5 ms, and the recycle delay was 0.3 s.

Results and Discussion

1. Experimental Information. The XRD pattern of as-synthesized $AlPO_4$-18 is characteristic of a material with a high crystallinity (Figure 2a). All diffraction peaks can be assigned to the *hkl* reflections of the reference compound, which indicates that the compound is pure and does not contain impurities. After calcination and subsequent rehydration, the pattern is modified, as already reported previously[23] (Figure 2b). The absence of broad signals in the region between 20 and 40° (2θ), characteristic of amorphous material, suggests that the crystallinity is retained upon hydration. Moreover, the complete reversibility of the hydration/dehydration process indicates that structure modifications are somewhat minor and do not involve bond cleavage with a reorganization of the framework. As already mentioned, attempts to index the powder pattern of the calcined-rehydrated $AlPO_4$-18 were unsuccessful. Simmen, who solved the structures of the calcined and as-synthesized dehydrated forms of the aluminophosphate, proposed an indexation with two different phases: a triclinic phase with $a = 9.29$, $b = 9.36$, $c = 18.46$ Å, $\alpha = 90.9$, $\beta = 96.5$, $\gamma = 90.9°$; and a monoclinic one with $a = 14.09$, $b = 12.83$, $c = 17.91$ Å, $\beta = 92.9°$.[61] Our pattern has been indexed using a triclinic cell with $a = 9.219$, $b = 9.335$, $c = 18.435$ Å, $\alpha = 90.883$, $\beta = 96.371$, $\gamma = 90.939°$. The cell parameters are very similar to those of the triclinic cell reported by Simmen. This cell indexes almost all experimental reflections between 8 and 26° (2θ) (part a and b of Figure 7). Only three weak diffraction peaks are omitted, but they could be indexed using a second monoclinic cell, as already proposed.[61] Despite the difficulties to index the pattern using a single cell, Simmen refined partially the pattern and proposed atomic coordinates. To simplify the refinement, water molecules were omitted, so all aluminum atoms remained tetrahedrally coordinated. Nevertheless, this structure can be regarded as a good approximation of the real structure and can be used as a starting model for theoretical calculations. The triclinic unit cell of the calcined rehydrated structure is not very different from that of the calcined dehydrated compound ($a = 9.355$, $b = 9.355$, $c = 18.570$ Å, $\alpha = 89.993$, $\beta = 89.993$, $\gamma = 85.755°$). So, the modifications of the structure resulting from the adsorption of water are somewhat minor. The situation was very similar in $AlPO_4$-34, and we can see that unit cell parameters of calcined-rehydrated $AlPO_4$-34 and $AlPO_4$-18 look similar, except that the *c*-axis value is doubled in the latter to account for the arrangement of D6R units.

The calcined-rehydrated form of $AlPO_4$-18 has been characterized by thermal analysis. A single weight loss, observed between room temperature and 70 °C, corresponds to the formula $AlPO_4 \cdot 2H_2O$. The same stoichiometry was found in $AlPO_4$-34, for which the hydrated unit cell contained 6 P, 6 Al, and 12 water molecules. However, the removal of water molecules from the **CHA** framework occurred in two well-separated steps. The first step, observed around room temperature, corresponds to the removal of one water molecule per unit cell. The other water molecules (11 H_2O) were expelled all together at higher temperatures (50−70 °C). Experimental studies combined with theoretical calculations have shown that the water molecule expelled at room temperature is located in D6R units of the **CHA** framework. The absence of weight loss around room temperature in the TGA curve of $AlPO_4$-18 is an indication that the hydrated framework does not contain water molecules in the D6R units. This specific position may be energetically or sterically favored in the **CHA** framework where all layers of D6R units are parallel.

The modification of the framework upon rehydration is clearly evidenced by ^{27}Al and ^{31}P MAS NMR. The ^{27}Al MAS spectrum is composed of signals characteristic of tetrahedrally and octahedrally coordinated aluminum atoms at ca. 40 and −15 ppm, respectively. By contrast to $AlPO_4$-34, the spectrum does not contain any contribution from pentacoordinated species. The AlO_4/AlO_6 ratio between tetrahedral and octahedral species can be estimated by integration of the different signals. From the spectrum in Figure 3, we obtain a ratio of 0.93, which suggests that the hydrated framework contains approximately the same number of 4- and 6-coordinate Al species. However, the relative intensities of NMR lines of quadrupolar nuclei are not always directly proportional to the concentration of the corresponding species. Under such conditions, the value of the AlO_4/AlO_6 ratio must be considered as an approximation, not as an exact value.

By contrast to $AlPO_4$-34, all crystallographically distinct Al sites could not be resolved using a 2D-5Q MAS NMR sequence. Only two types of 4-coordinate and two types of 6-coordinate species are clearly evidenced in the isotropic dimension. Satyanarayana et al.[62] have reported the 2D-3Q MAS NMR spectrum of calcined rehydrated $AlPO_4$-18. They observed two intense signals in the tetrahedral region along with a weak resonance with an isotropic chemical shift at ca. 56 ppm. The very low intensity of the latter was attributed to the poor multiquanta excitation efficiency, due to a large quadrupolar interaction. Such a weak signal around 56 ppm was not observed in the 2D-5Q MAS spectra of our rehydrated compound. The resolution of one-dimensional spectra as well as that of X-ray diffraction patterns shows that the absence of signal cannot be attributed to a low crystallinity. Other reasons can be involved like the difference in magnetic field or the multiquanta excitation efficiency. However, the same pulse sequence applied to

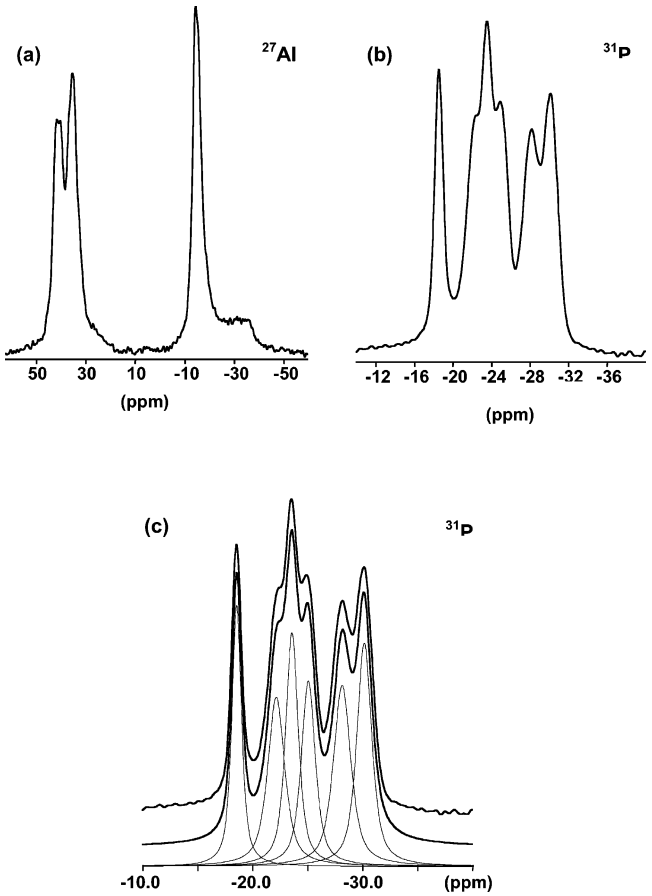

Figure 3. MAS NMR ^{27}Al (a) and ^{31}P (b); deconvolution of ^{31}P signal (c).

different aluminophosphates allowed us to resolve broad signals, with large quadrupolar coupling constant (C_Q) values. So, the existence of a third signal in the tetrahedral region of the spectrum of calcined-rehydrated $AlPO_4$-18 is still a matter of debate. The two tetrahedral sites possess relatively small C_Q values (1.92 and 2.13 MHz, respectively), characteristic of quite regular AlO_4 tetrahedra. By contrast, one of the 6-coordinate species possesses a high C_Q value (5.9 MHz), suggesting that the corresponding octahedron is strongly distorted.

More information about the coordination of water molecules in the framework has been obtained by ^{27}Al−^{31}P CP/MAS NMR correlation spectroscopy (HETCOR). This technique is based on a polarization transfer between ^{27}Al and ^{31}P nuclei through dipolar interactions. The transfer decreases very rapidly with the distance around Al atoms. So, it is limited to neighboring P atoms, typically those in the first coordination sphere. Correlation peaks in the 2D spectrum are thus a direct picture of framework connectivities. Theoretically, the intensity of a correlation signal is proportional to the number of Al atoms around P. However, the intensity also depends on the distance, on the contact time and on the efficiency of the cross-polarization transfer, which makes the method not directly quantitative. The ^{27}Al−^{31}P CP/MAS NMR correlation spectrum of calcined rehydrated $AlPO_4$-18 is shown in Figure 4. To clarify the assignment of the different signals, ^{31}P NMR lines have been numbered from 1 to 6. Correlation peaks with ^{27}Al chemical shifts around −10 ppm in the f_1 dimension can be assigned to P atoms bonded to 6-coordinate Al. On the other hand, signals with a projection around 40 ppm in the indirect dimension indicate the existence of chemical bonds between P atoms and AlO_4 tetrahedra. Thus, it is possible to estimate the

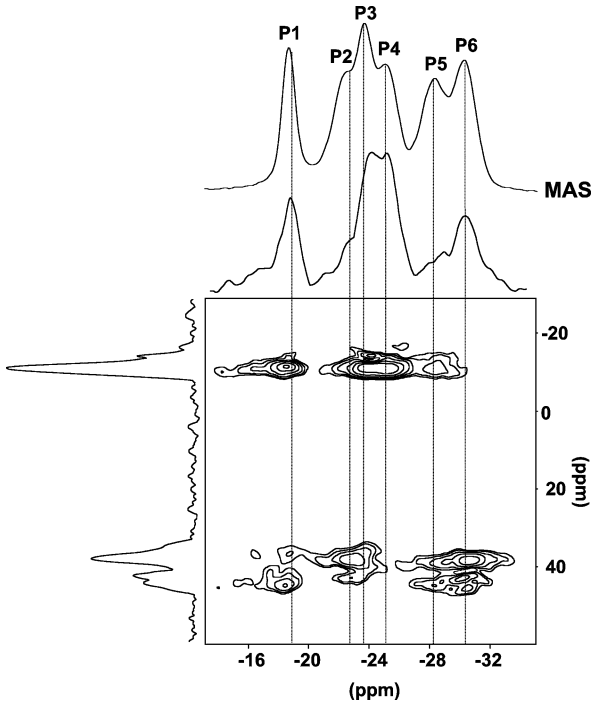

Figure 4. ^{27}Al−^{31}P CP MAS HETCOR NMR spectra of hydrated $AlPO_4$-18 (*x* axis, ^{31}P; *y* axis, ^{27}Al).

number of AlO_4 and AlO_6 polyhedra around all P atoms, corresponding to signals 1−6 in the one-dimensional spectrum.

In general, the complexity of the 2D spectrum is such that there is not a unique solution and several connectivity schemes can be proposed. As an example, species P6 in Figure 4 is strongly correlated to AlO_4 tetrahedra but weakly to AlO_6 octahedra. A magnification of the signal shows that a correlation peak exists between P6 and AlO_6 species, but with a very low intensity. The ^{27}Al 2D-5Q MAS spectrum has revealed the existence of distorted AlO_6 octahedra, with strong quadrupolar coupling constants. The polarization transfer from such species is difficult, and this may explain the absence of correlation between P6 and Al octahedra in the HETCOR spectrum. Finally, two propositions of framework connectivity for phosphorus have been retained and are given in Table 1.

In the first proposition, we have assumed that a very weak signal can be interpreted as an absence of chemical bonding. In the second one, we have taken into account that the polarization transfer efficiency can be low for certain species, leading to weak correlation peaks. Note that the two propositions are quite similar and that they differ only by the connectivities around P4 and P6.

2. Approach from First-Principles Calculations. To perform a structural search for the hydrated $AlPO_4$-18 from first-principles calculations, a hypothesis is required on the symmetry and unit cell of the AlPO framework. Two possible routes have been followed here and they will be sequentially presented.

2.1. From the Structure of Dehydrated $AlPO_4$-18. The first approach consists of starting with the known structure of the dehydrated $AlPO_4$-18, as an extension of the methodology previously used on $AlPO_4$-34. The DFT-optimized structure of the dehydrated $AlPO_4$-18 is in very good agreement with the experimental refinement with a slight overestimation of unit cell vector length (1.4%) and an average quadratic difference in the atomic positions of only 0.053 Å. Hydration studies were performed using the experimental unit cell of the dehydrated aluminophosphate as a starting structure.[34] The unit cell of the dehydrated aluminophosphate is indeed a natural starting point,

TABLE 1: Two Propositions of Framework Connectivity for the Six Nonequivalent Phosphorus Atoms

	P1	P2	P3	P4	P5	P6
prop. 1	$2AlO_6$, $2AlO_4$	$1AlO_6$, $3AlO_4$	$3AlO_6$, $1AlO_4$	**$4AlO_6$**	$2AlO_6$, $2AlO_4$	**$4AlO_4$**
prop. 2	$2AlO_6$, $2AlO_4$	$1AlO_6$, $3AlO_4$	$3AlO_6$, $1AlO_4$	**$3AlO_6$, $1AlO_4$**	$2AlO_6$, $2AlO_4$	**$1AlO_6$, $3AlO_4$**

which we considered first. It is formed by a supercell containing four channels, with a R3r space group. The symmetry was not taken into account in the theoretical study, and hence a P-1 group was used. It was not possible to obtain a single channel unit cell (similar to $ALPO_4$-34) yielding a good agreement with the NMR results. Following the analysis of the experimental data, 48 H_2O molecules should be positioned in the unit cell of the porous network, 24 in direct interaction with the Al atoms and the other 24 forming the hydrogen bond network in the channels. The final unit cell is rather large with 288 atoms (144 from the $AlPO_4$ framework and 144 from the water molecules). The initial distribution of H_2O molecules was inferred from the analysis of the NMR HETCOR 2D spectrum, choosing the first proposition of assignment in terms of environment of phosphorus. The second assignment was not considered since it leads to several structural possibilities, which is difficult from the computational aspect with such a large unit cell. The density of water molecules was kept constant in the channels, but to be able to conform to the NMR results, a different repartition between coordinated and channel water molecules was used. This initial structure shows two main drawbacks. First, the distribution is not symmetric in the upper and lower channels of the cell, originally equivalent in the dehydrated structure. The upper channel contains 8 H_2O molecules coordinated to the Al atoms and 16 distributed in the channel, while the lower channel shows the opposite repartition. Second, the geometry of the octahedral Al atoms is far from correct, since it is derived from the tetrahedral environment in the dehydrated structure by simply positioning two additional H_2O molecules. An important relaxation is hence required to accommodate the hexacoordinate Al.

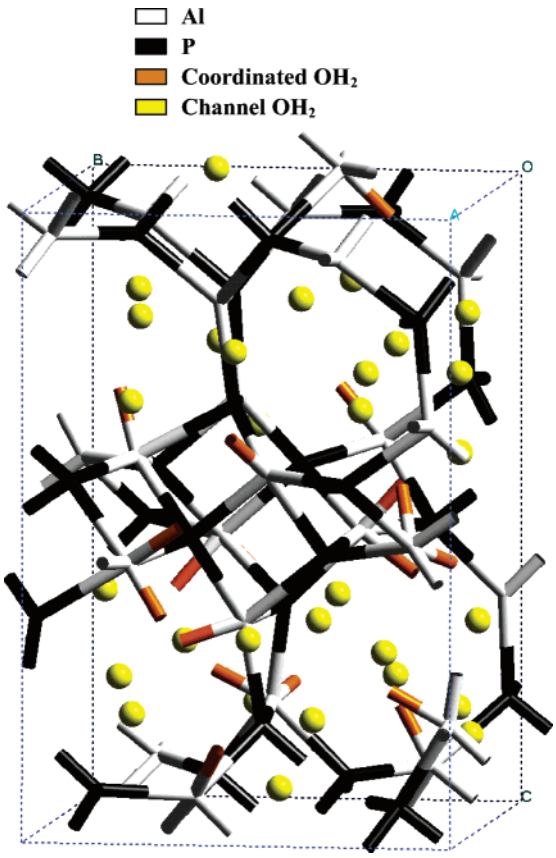

Figure 5. Calculated hydrated structure I, with the dehydrated $AlPO_4$-18 unit cell as a starting point (48 water molecules, 288 atoms total in the cell). Framework Al (resp P) atoms are shown as white (black) sticks, water molecules coordinated to Al are shown as orange sticks, while those positioned in the channel by hydrogen bonds are indicated by yellow balls. Hydrogen atoms are omitted for clarity.

To avoid a highly probable initial decoordination of the H_2O molecules due to incorrect Al geometry, the relaxation was performed in two steps. A first step, in which H_2O molecules were fixed to allow a local relaxation of the Al atoms, was followed by a second step in which all atoms were free to relax. Finally the unit cell parameters were modified to the values reported by Simmen for the hydrated structure.[34] To better probe the configuration space, the geometry relaxation was followed by a molecular dynamic run of 1.25 ps and again by a zero-temperature relaxation. The best structure obtained following this approach is given in Figure 5 (structure I). Despite all precautions taken during relaxation, 6 water molecules left the coordination sphere of aluminum and only 18 molecules remained bonded to Al atoms. In the unit cell, 12 Al atoms are hydrated: 6 of them by two H_2O molecules (octahedral Al) and the other 6 by only 1 H_2O molecule (pentahedral Al). The hydration process is thus incomplete in disagreement with experimental data. Indeed, thermal analysis concluded that the unit cell of the calcined rehydrated $AlPO_4$-18 contains 24 H_2O molecules, and NMR revealed the absence of 5-coordinate Al species. Even if one supposes that 5-fold Al atoms are in course of hydration and will form octahedral sites for longer simulations, the obtained connectivity for the P atoms does not agree with NMR data. So, this approach is not satisfactory, mainly because of an incomplete hydration process, that could arise either from a too large available volume for H_2O in the cavity (in other words too small water density) or from an underestimation from DFT-GGA of the binding energy of H_2O with the Al framework atoms. This could also be explained by the initial nonsymmetric repartition of coordinated and channel water molecules in the channels of the unit cell, from the constraint of the first NMR assignment. To go beyond this first attempt, instead of exploring multiple possibilities for the large unit cell, another route has been followed.

2.2. From a Partial Refinement of Hydrated $AlPO_4$-18. The starting unit cell is now that obtained by Simmen[61] and Meden[63] after a partial Rietveld refinement of the pattern of the hydrated $AlPO_4$-18. Only the framework oxygen and aluminum atoms have included in this Rietveld determination, the water molecules being omitted. As a consequence, all Al atoms are in a tetrahedral environment. The resulting unit cell, with a P-1 symmetry, is half the previous one, with 72 framework AlPO atoms and 24 water molecules in the channels. However none of these H_2O molecules was included in the structural search, which considered only the AlPO framework atoms and constrained all Al atoms in a unique tetrahedral environment. Hence, again, some of the aluminum atoms have to change their geometry from tetrahedral to octahedral to account for the presence of additional water molecules. Since no structural information is available for H_2O molecules, the two channels of the unit cell were considered as equivalent and each of them was filled with 12 randomly distributed water molecules (Figure 6a). No initial hypothesis was made on the

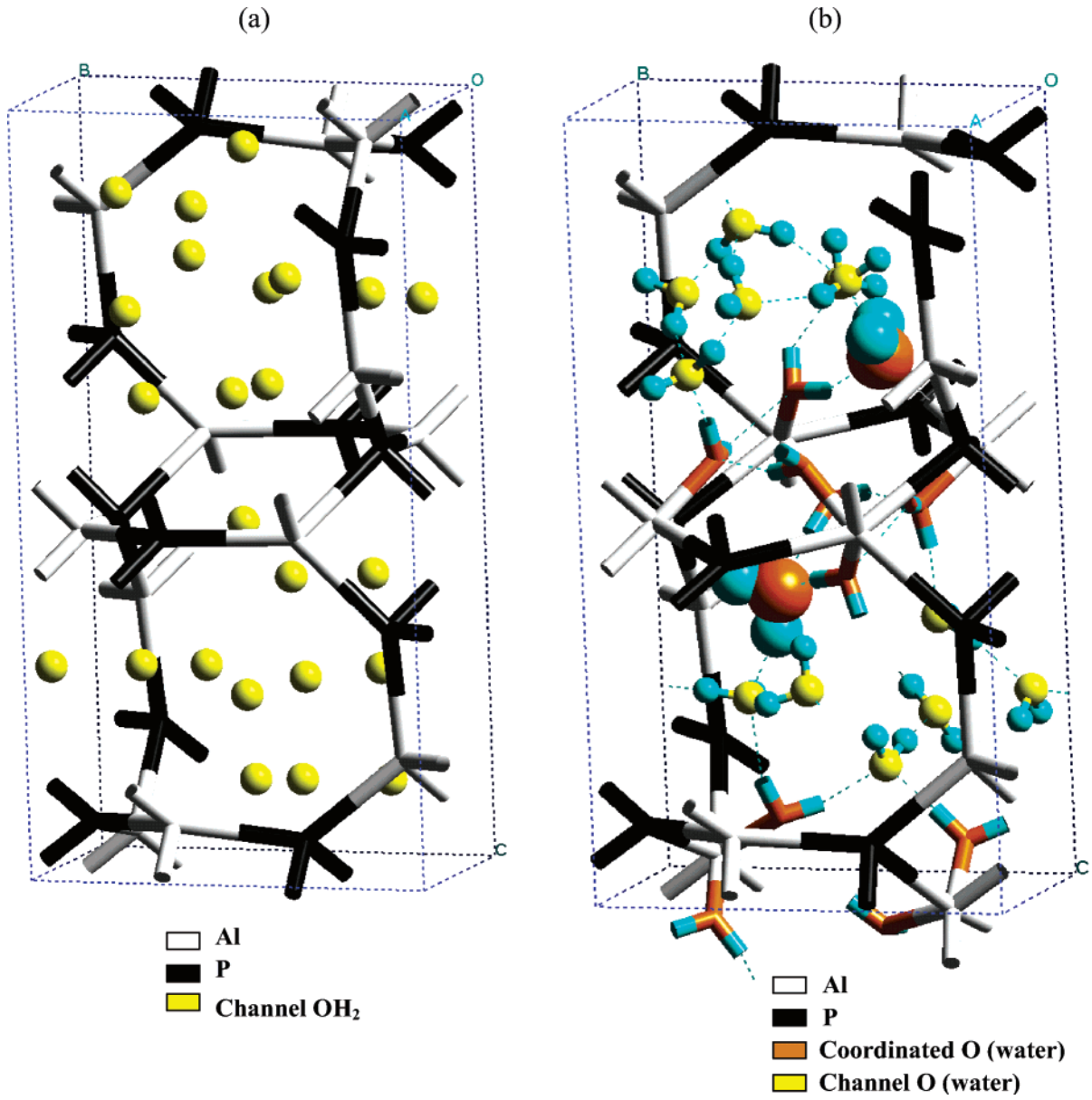

Figure 6. Calculated hydrated structure II, with the partial refinement of hydrated $AlPO_4$-18 unit cell as a starting point (24 water molecules, 144 atoms in the cell): (a) initial configuration for the simulation (24 water molecules); framework Al (resp P) atoms as white (black) sticks, water molecules as yellow balls. (b) Optimized hydrated $AlPO_4$-18 structure II; framework Al (resp P) atoms as white (black) sticks, oxygen of coordinated water molecules as orange sticks, oxygen atoms of channel water molecules as yellow balls, hydrogen atoms as blue balls. Two specific water molecules are displayed with large balls (see text) and hydrogen bonds with a blue dotted line.

environment of the 12 Al atoms in the cell, none of them being in direct interaction with H_2O molecules.

To explore all possible configurations for H_2O molecules in the channels, a simple geometry optimization is not enough, since several energy minima exist on the potential-energy surface. This is especially the case when the initial configuration is far from the optimal one. Here, our approach is similar to that followed for the adsorption of hydrocarbon molecules in acidic zeolites.[64] Molecular dynamics (MD) and geometry optimization runs are alternated. After a short MD simulation, a zero-temperature relaxation is performed to favor the coordination of H_2O molecules that are in the vicinity of an Al atom. Another MD is then set to explore the configurations for the other molecules in the channel. To accelerate the formation of octahedral Al atoms, H_2O molecules in the vicinity of 5-coordinate Al atoms are systematically moved near it, at a distance corresponding to an Al−O bond distance. After four steps in this cycle, all of them leading to a decrease of the total energy, a structure with 12 H_2O molecules coordinated to Al atoms is obtained and shown in Figure 6b (structure II). The 12 molecules (with the O atom shown in orange on the figure) are bonded to 6 octahedrally coordinated Al atoms, the 6 other Al remaining in a tetrahedral coordination. The detailed coordinates for this structure are given in Appendix 1. The Al−O distance ranges from 1.9 to 2.3 Å, except for the $Al_{11}-O_{76}$ and Al_5-O_{95} bonds (water molecules shown as large balls in Figure 6b) that are slightly larger (4.1 and 3.6 Å, respectively), since these molecules are engaged in a strong hydrogen bond interaction.

This second structure II agrees quite well with available experimental data:

(i) The P-1 symmetry is conserved for the $AlPO_4$ framework atoms, despite the fact that this is not the case for the H_2O molecules in the channels.

(ii) The repartition of H_2O molecules (12 coordinated to Al, 12 forming a H bond network) implies that both channels are

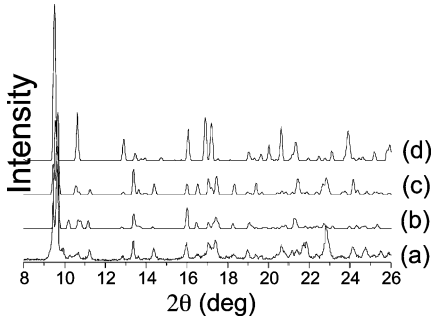

Figure 7. X-ray diffraction powder patterns: (a) experimental one of calcined rehydrated $AlPO_4$-18, (b) simulated one of the partial refinement procesed by Meden[62] (with only the 72 framework atoms), (c) simulated from the optimized structure II, (d) simulated from the optimized structure I.

equivalent, as it is the case in the as-made and calcined dehydrated forms of $AlPO_4$-18.

(iii) The distribution of Al atoms, in particular the absence of 5-coordinate species and an equal number of octahedral and tetrahedral species, agrees with NMR.

(iv) The environment of phosphorus (4 P atoms surrounded by $3AlO_6$ and $1AlO_4$, 4 P atoms surrounded by $2AlO_6$ and $2AlO_4$, and 4 P atoms surrounded by $1AlO_6$ and $3AlO_4$) agrees with the second proposition derived from the analysis of the HETCOR NMR spectrum.

Figure 7 compares the experimental X-ray diffraction powder pattern of calcined rehydrated $AlPO_4$-18 with those of structures I and II. Clearly, the agreement between experimental and calculated patterns is better for the second structure containing 144 atoms. Although peak positions are reasonably good between 8 and 26° (2θ), some of the intensities are not well reproduced. Patterns cannot match perfectly because the indexation was not correct, even before optimization. Nevertheless, structure II appears to be a good description of the real structure of the calcined-rehydrated aluminophosphate. As already mentioned, the hydrated solid is certainly more complex and could be a mixture of two structures in which structure II predominates.

Conclusion

We have proposed a combined experimental-theoretical approach to determine the structure of hydrated $AlPO_4$-18. Besides a detailed analysis of TGA and NMR results, a combination of DFT geometry optimization and molecular dynamics gives important insights on the structure of H_2O molecules in the channels of the hydrated aluminophosphate. The simulated structure perfectly agrees with TGA and NMR information. However the agreement with the powder X-ray pattern is not so perfect, suggesting a more complex situation, possibly a mixture of structures. Previous theoretical studies on $AlPO_4$-34 have shown that the X-ray spectrum is mainly sensitive to the structure of the AlPO framework and only marginally to the positions of H_2O molecules. This is not the case for NMR, which gives local information on the aluminum sites, directly influenced by the position and coordination of the H_2O molecules. The example of $AlPO_4$-18 clearly shows the difficulty to access the detailed structure of a hydrated aluminophosphate framework when the powder pattern is not perfectly indexed.

Acknowledgment. We thank A. Meden for helpful discussions, and we acknowledge IDRIS at CNRS for the attribution of CPU time under Project 0609.

Supporting Information Available: Structure parameters and atomic crystallographic coordinates for the optimized structure of calcined-rehydrated $AlPO_4$-18 (cell with 144 atoms, structure II). This material is available free of charge via the Internet at http://pubs.acs.org.

References and Notes

(1) Wilson, S. T.; Lok, B. M.; Messina, C. A.; Cannan, T. R.; Flanigen, E. M. *J. Am. Chem. Soc.* **1982**, *104*, 1146.
(2) Wilson, S. T.; Lok, B. M.; Flanigen, E. M. U.S. Pat. 4,310,440, 1982.
(3) Flanigen, E. M.; Lok, B. M.; Patton, R. L.; Wilson, S. T. *Stud. Surf. Sci. Catal.* **1986**, *28*, 103.
(4) Hartmann, M.; Kevan, L. *Chem. Rev.* **1999**, *99*, 635.
(5) Thomas, J. M. *Angew. Chem., Int. Ed.* **1999**, *38*, 3588.
(6) Bennett, J. M.; Dytrych, W. J.; Pluth, J. J.; Richardson, J. W., Jr.; Smith, J. V. *Zeolites* **1986**, *6*, 349.
(7) Oliver, S.; Kuperman, A.; Ozin, G. A. *Angew. Chem., Int. Ed.* **1998**, *37*, 46.
(8) Blackett, C. S.; Patton, R. L. *J. Phys. Chem.* **1984**, *88*, 6135.
(9) Muller, D.; Gessner, W.; Berhens, H. J.; Scheler, G. *Chem. Phys. Lett.* **1981**, *79*, 59.
(10) Kustanovich, I.; Goldfarb, D. *J. Phys. Chem.* **1991**, *95*, 8818.
(11) Loshe, U.; Noack, M.; Jahn, E. *Ads. Sci. Technol.* **1986**, *3*, 19.
(12) Muller, D.; Jahn, E.; Fahlke, B.; Ladwig, G.; Hanbenreisser, U. *Zeolites* **1988**, *5*, 53.
(13) Anderson, M. W.; Sulikowski, B.; Barrie, P. J.; Klinowski, J. *J. Phys. Chem.* **1990**, *94*, 2730.
(14) Davis, M. E.; Saldarriaga, C.; Montes, C.; Garces, Y.; Crowder, C. *Nature* **1988**, *331*, 698.
(15) Wu, Y.; Chmelka, B. F.; Pines, A.; Davis, M. E.; Grobet, P. J.; Jacobs, P. A. *Nature* **1990**, *346*, 550.
(16) Davis, M. E.; Montes, C.; Hathaway, P. E.; Arhanet, J. P.; Hasha, D. L.; Garces, J. M. *J. Am. Chem. Soc.* **1989**, *111*, 3919.
(17) Kenny, M. B.; Sing, K. S. W.; Theocharis, C. R. *J. Chem. Soc., Chem. Com.* **1991**, 974.
(18) Khouzami, R.; Coudurier, G.; Lefebvre, F.; Vedrine, J. C.; Mentzen, B. F. *Zeolites* **1990**, *10*, 183.
(19) Meinhold, R. H.; Tapp, N. J. *J. Chem. Soc., Chem. Commun.* **1990**, 219.
(20) Peeters, M. P. J.; de Haan, J. W.; van de Ven, L. J. M.; van Hooff, J. H. C. *J. Phys. Chem.* **1993**, *97*, 5363.
(21) Tuel, A.; Caldarelli, S.; Meden, A.; McCusker, L. B.; Baerlocher, C.; Ristic, A.; Rajic, N.; Mali, G.; Kaucic, V. *J. Phys. Chem. B* **2000**, *104*, 5697.
(22) Hartmann, M.; Prakash, A. M.; Kevan, L. *J. Chem. Soc., Faraday Trans.* **1998**, *94*, 723.
(23) Caldarelli, S.; Meden, A.; Tuel, A. *J. Phys. Chem. B* **1999**, *103*, 5477.
(24) Goepper, M.; Guth, F.; Delmotte, L.; Guth, J. L.; Kessler, H. *Proceedings of the 8th International Zeolite Conference, Zeolites: Facts, Figures, Future*; Jacobs, P. A., van Santen, R. A., Eds.; Elsevier: Amsterdam, 1989; p 857.
(25) Briends, M.; Shikholeslami, A.; Peltre, M. J.; Delafosse, D.; Barthomeuf, D. *J. Chem. Soc., Dalton Trans.* **1989**, 1361.
(26) Parlitz, B.; Lohse, U.; Schreier, E. *Microporous Mater.* **1994**, *2*, 223.
(27) Briends, M.; Vomxchield, R.; Peltre, M. J.; Man, P. P.; Barthomeuf, D. *J. Phys. Chem.* **1995**, *99*, 8270.
(28) Smith, L.; Cheetham, A. K.; Morris, R. E.; Marchese, L.; Thomas, J. M.; Wright, P. A.; Chen, J. *Science* **1996**, *271*, 799.
(29) Zanjanchi, M. A.; Rashidi, M. K. *Spectrochim. Acta, A* **1999**, *55*, 947.
(30) Poulet, G.; Sautet, P.; Tuel, A. *J. Phys. Chem. B* **2002**, *106*, 8599.
(31) Chang, Y. F.; Vaughn, S. N.; Martens, L. R. M.; Soled, S. L.; Clem, K. R.; Baumgartner, J. E. U.S. Pat. 6,440,894, 2002.
(32) Chen, J.; Thomas, J. M. *J. Chem. Soc., Chem. Commun.* **1994**, 630.
(33) Janssen, M. J. G.; Verberckmoes, A.; Mertens, M. M.; Bons, A. J.; Mortier, W. J. U.S. Pat. 924,016, 2002.
(34) Simmen, A.; McCusker, L. B.; Baerlocher, C.; Meier, W. M. *Zeolites* **1991**, *11*, 654.
(35) He, H.; Klinowski, J. *J. Phys. Chem.* **1993**, *97*, 10385.
(36) Jänchen, J.; Peeters, M. P. J.; de Haan, J. W.; van de Ven, L. J. M.; van Hooff, J. H. C. *J. Phys. Chem.* **1993**, *97*, 12042.
(37) Izmailova, S. G.; Vasiljeva, E. A.; Karetina, I. V.; Feoktistova, N. N.; Khvoshchev, S. S. *J. Colloid Interface Sci.* **1996**, *179*, 374.
(38) Kresse, G.; Hafner, J. *Phys. Rev. B* **1993**, *47*, 5858.
(39) Kresse, G.; Hafner, J. *Phys. Rev. B* **1993**, *48*, 13115.
(40) Kresse, G.; Hafner, J. *Phys. Rev. B* **1994**, *49*, 14251.
(41) Kresse, G.; Furthmüller, J. *Comput. Mater. Sci.* **1996**, *6*, 15.
(42) Kresse, G.; Furthmüller, J. *Phys. Rev. B* **1996**, *54*, 11169.

(43) Perdew, J. P.; Zunger, A. Phys. Rev. B **1981**, *23*, 5048.
(44) Perdew, J. P. In *Electronic Structure of Solids 91*; Ziesche, P., Eschrig, H., Eds.; Akademic verlag: Berlin, 1991; p 11.
(45) Perdew, J. P.; Burke, K.; Wang, Y. *Phys. Rev. B* **1996**, *54*, 16533.
(46) Kresse, G.; Joubert, J. *Phys. Rev. B* **1999**, *59*, 1758.
(47) Blöch, P. E. *Phys. Rev. B* **1994**, *50*, 17953.
(48) Payne, M. C.; Teter, M. P.; Allan, D. C.; Arias, T. A.; Joannopoulos, J. D. *Rev. Mod. Phys.* **1992**, *64*, 1045.
(49) Poulet, G.; Sautet, P.; Artacho, E. *Phys. Rev. B* **2003**, *68*, 75118.
(50) Nosé, S. *J. Chem. Phys.* **1984**, *81*, 511.
(51) Nosé, S. *Prog. Theor. Phys. Suppl.* **1991**, *103*, 1.
(52) Allen, M. P.; Tidesley, D. J. *Computer Simulations of liquids*; Clarendon: Oxford, 1987.
(53) Yvon, K.; Jeitschko, W.; Parthe, E. *J. Appl. Crystallogr.* **1977**, *10*, 73.
(54) Wu, G.; Rovnyak, D.; Griffin, R. G. *J. Am. Chem. Soc.* **1996**, *118*, 9326.
(55) Caldarelli, S.; Ziarelli, F. *J. Am. Chem. Soc.* **2000**, *122*, 12015.
(56) Pines, A.; Gibby, M. G.; Waugh, J. S. *J. Chem. Phys.* **1973**, *59*, 569.
(57) Marion, D.; Würthrich, K. *Biochem. Biophys. Res. Commun.* **1983**, *113*, 967.
(58) Drobny, G.; Pines, A.; Sinton, S.; Weitekamp, D.; Wemmer, D. *Symp. Faraday Div. Chem. Soc.* **1979**, *13*, 49.
(59) Hartmann, S. R.; Hahn, E. *Phys. Rev.* **1962**, *128*, 2042.
(60) Peersen, O. B.; Wu, X. L.; Kustanovitch, J.; Smith, S. O. *J. Magn. Res., Ser. A* **1993**, *104* (A), 334.
(61) Simmen, A. Thesis, University of Zürich, ETH No. 9710, Switzerland, 1992.
(62) Satyanarayana, C. V.; Gupta, R.; Damodarah, K., Sivasanker, S.; Ganapathy, S. *Stud. Surf. Sci. Catal.* **2001**, *135*, 2098.
(63) Meden, A. Private communication.
(64) Benco, L.; Demuth, T.; Hafner, J.; Hutschka, F.; Toulhoat, H. *J. Catal.* **2002**, *205*, 147.